References

1) United States Pharmacopoeia 28, pp. 3029-3031 (2006)
2) 3 June 2003, Iyaku-shin Hatsu No. 0603001, Iyaku-kyoku Shinsakanri-Kachou Tsuuchi「Anteisei-shiken Guideline no Kaitei ni tsuite」
3) Kato, F., M. Otsuka and Y. Matsuda: "Kinetic Study of the Transformation of Mefenamic Acid Polymorphs in Various Solvents and under Humidity Conditions", *Int. J. Pharm.*, **321**, 18-26 (2006)
4) Matsuda, Y. and R. Teraoka: "Photostability of Solid-State Ubidecarenone at Ordinary and Elevated Temperatures under Exaggerated Irradiation", *J. Pharm. Sci.*, **72**, 1198-1203 (1983)
5) Teraoka, R., Y. Konishi and Y. Matsuda: "Photochemical and Oxidative Degradation of the Solid-State Tretinoin Tocoferil", *Chem. Pharm. Bull.*, **49**, 368-372 (2001)
6) Teraoka, R. and Y. Matsuda: "Stabilization-oriented Preformulation Study of Photolabile Menatetrenone (Vitamin K_2)", *Int. J. Pharm.*, **93**, 85-90 (1993)
7) Matsuda, Y., R. Teraoka and I. Sugimoto: "Comparative Evaluation of Photostability of Solid-State Nifedipine under Ordinary and Intensive Light Irradiation Conditions", *Int. J. Pharm.*, **54**, 211-221 (1989)
8) Genton, D. and U. W. Kesselring: "Effect of Temperature and Relative Humidity on Nitrazepam Stability in Solid State", *J. Pharm. Sci.*, **66**, 676-680 (1977)
9) Plotkowiak, Z.: "The Effect of the Chemical Character of Certain Penicillins on the Stability of β-lactam Group in Their Molecules, Part 7: Effect of Humidity in the Solid State", *Pharmazie*, **44**, 837-839 (1989)
10) Yoshioka, S. and M. Uchiyama: "Nonlinear Estimation of Kinetic Parameters for Solid-state Hydrolysis of Water-soluble Drugs", *J. Pharm. Sci.*, **75**, 459-462 (1986)
11) Kakinoki, K., K.Yamane, R. Teraoka, M. Otsuka and Y. Matsuda: "Effect of Relative Humidity on the Photocatalytic Activity of Titanium Dioxide and Photostability of Famotidine", *J. Pharm. Sci.*, **93**, 582-589 (2004)
12) Kakinoki, K., K. Yamane, M. Yamamoto, R. Teraoka, S. Sugimoto and Y. Matsuda: "Effect of Titanium Dioxide on Photostability of Solid-state Mequitazine", *Chem. Pharm. Bull.*, **53**, 1092-1096 (2005)
13) Matsuda, Y. and R. Teraoka': "Comparative Evaluation of Coloration of Photosensitive Solid Drugs under Variuos Light Sources", *YAKUGAKU ZASSHI*, **100**, 953-957 (1980)
14) Matsuda, Y., R. Akazawa, R. Teraoka and M. Otsuka: "Pharmaceutical Evaluation of Carbamazepine Modifications: Comparative Study for Photostability of Carbamazepine Polymorphs by using Fourier-transformed Reflection-absorption Infrared Spectroscopy and Colorimetric Measurement", *J. Pharm. Pharmacol.*, **46**, 162-167 (1994)
15) Connors, K. A., G. L. Amidon and L. Kennon ed.: "Chemical Stability of Pharmaceuticals", pp. 88-89, Willey & Sons, New York (1979)
16) De Villiers, M. M., J. G. van der Watt and A. P. Lotter: "Kinetic Study of the Solid-State Photolytic Degradation of Two Polymorphic Forms of Furosemide", *Int. J. Pharm.*, **88**, 275-283 (1992)
17) Sugimoto, I., K. Tohgo, K.Sasaki, H. Nakagawa, Y. Matsuda and R. Masahara: *YAKUGAKU ZASSHI*, **101**, 1149-1153 (1981)
18) Teraoka, R., M.Otsuka and Y.Matsuda: "Evaluation of Photostability of Solid-State Dimethy 1, 4-dihydro-2, 6-dimethyl-4-(2-nitro-phenyl)-3, 5-pyridine dicarboxylate by using Fourier-transformed Reflection-absorption Infrared Spectroscopy", *Int. J. Pharm.*, **184**, 35-43 (1999)
19) Matsuda, Y. and E. Tatsumi: "Physicochemical Characterization of Furosemide Modifications", *Int. J. Pharm.*, **60**, 11-26 (1990)
20) Kojima, T., S.Onoue, F.Kato, R.Teraoka, Y.Matsuda and S.Kitagawa: "Effect of Spectroscopic Properties on Photostability of Tamoxifen Citrate Polymorphs", *Int. J. Pharm.*, in press (2007)
21) Teraoka, R., M.Otsuka and Y.Matsuda: "Evaluation of Photostability of Solid-state Nicardipine Hydrochloride Polymorphs by using Fourier-transformed Reflection-absorption Infrared Spectroscopy-Effect of Grinding on the Photostability of Crystal Form", *Int. J. Pharm.*, **286**, 1-8 (2004)
22) Matsuda, Y.: "Some Aspects on the Evaluation of Photostability of Solid-State Drugs and Pharmaceutical Preparations", *PHARM TECH JAPAN*, **10**, 739-749 (1994)
23) Matsuda, Y. and R. Teraoka: "Some Stabilization Designs for Photolabile Drugs in Solid Dosage Forms", *PHARM TECH JAPAN*, **22**, 1963-1971 (2006)

Available online at www.sciencedirect.com

ScienceDirect

Journal of Chromatography A, 1142 (2007) 231–235

JOURNAL OF CHROMATOGRAPHY A

www.elsevier.com/locate/chroma

Short communication

Determination of biotin following derivatization with 2-nitrophenylhydrazine by high-performance liquid chromatography with on-line UV detection and electrospray-ionization mass spectrometry

Chikako Yomota*, Yukiko Ohnishi

National Institute of Health Sciences, 1-18-1 Kamiyoga, Setagaya-ku, Tokyo 158-8501, Japan

Received 7 February 2006; received in revised form 13 December 2006; accepted 15 December 2006
Available online 21 December 2006

Abstract

Currently, biotin is typically determined in Japan using a microbiological method. Such microbiological assays are sensitive, but they are not always highly specific and are also rather tedious and time-consuming. In the present study, RP-HPLC and LC–MS methods for the determination of biotin have been developed by derivatizing the carboxyl group with 2-nitrophenylhydrazine hydrochloride. 2-Nitrophenylhydrazine is used for the derivatization of carboxylic acids, and these derivatives are known to be applicable to LC–MS detection. Biotin in tablets were extracted by the addition of water and ultrasonic agitation. In order to clean up the sample solution, the filtrate was applied to an ODS cartridge and eluted with methanol. The conditions for preparing the 2-nitrophenylhydrazide derivatives were modified from a previous report for fatty acids. Good recovery rates of over 70% were obtained for the addition of 5–125 μg of biotin per formulation. The detection limit in HPLC at 400 nm was 0.6 ng per injection, with good linearity being obtained over the concentration range 0.001–0.2 μg per injection. Further, derivatives were determined by LC–MS with electrospray ionization, where the spectra indicated the molecular ions $[M+H]^+$. The detection limit was 0.025 ng per injection in the selected ion monitoring analysis, and linearity was observed in the range of 0.6–6 ng per injection. The proposed method could be used to specifically determine the presence of biotin in relatively clean samples.

Keywords: Biotin; 2-Nitrophenylhydrazine derivative; HPLC; LC–MS; Electro spray ionization

1. Introduction

Biotin (vitamin H) is a coenzyme essential in amino acid metabolism and in the maintenance of skin, hair and nerves. Low biotin intake has been reported to result in serious biochemical disorders, such as reduced carboxylase activity, inhibition of protein and RNA synthesis and reduced antibody production. In recent years, the interest in this vitamin has increased, mainly due to diseases such as multiple carboxylase deficiency, which can be successfully treated by biotin administration. A decrease in biotin status has been reported to occur in several population groups, such as pregnant women.

In Japan, in 2001, the nutritional requirement of 30 μg of biotin per day was set for adults and 5 μg for infants, with an additional requirement of 5 μg for pregnant women. Three years later, biotin was also approved as a food additive and now can be supplied as ingredient in food with nutrient function claims [1].

Diagnosis of biotin deficiency is crucial as well as the monitoring of biotin levels in biological fluids of patients receiving biotin treatment. It is also important to determine biotin levels in pharmaceutical preparations as well as in food and food supplement products, which constitute the main source of biotin for humans. For this reason, analytical methods have been developed, in order to determine biotin in biological fluids, as well as in various types of food products and pharmaceutical preparations containing biotin [2].

Biotin has long been determined by a microbiological method, which is tedious and time-consuming [3]. Recently, various HPLC methods have been described to improve the selectivity [4–9]. Using 4-bromomethylmethoxycoumarin [4], 9-anthryldiazomethane (ADAMS) [5,6], and 1-pyrenyldiazomethane (PDAM) [7] as pre-column reagents, biotin was derivatized and determined by fluorometric detection. However

* Corresponding author. Tel.: +81 3 3700 1141; fax: +81 3 3707 6950.
E-mail address: yomota@nihs.go.jp (C. Yomota).

0021-9673/$ – see front matter © 2006 Elsevier B.V. All rights reserved.
doi:10.1016/j.chroma.2006.12.058

they are still inappropriate for common analysis, due to a lack of sensitivity or their complicated procedure or the many unknown peaks derived from reagents. Kamata et al. reported a method of applying electrochemical detection to determine biotin in multivitamin pharmaceutical preparations [8], and achieved a good separation. Further, biotin methylester was described as being well detected by MS detection in a positive ion chemical ionization mode [9]. Wolf et al., reported the quantification of biotin in human skin using LC–MS and resulted in the detection limit of 0.8 ng/mL [10]. Recently, LC–MS/MS analysis of biotin was also reported to be applicable to food samples with a biotin content over 100 μg/kg [11].

On the other hand, it was demonstrated in some reports that aliphatic acids and organic acids reacted selectively with 2-nitrophenylhydrazine hydrochloride (2-NPH·HCl), and produced derivatives that are UV detectable [12–15]. The main advantage of derivatization with hydrazines, using coupling reagent 1-ethyl-3-(3-dimethylaminopropyl)-carbodiimide hydrochloride (EDC·HCl), with respect to other derivatization reagents is that the reaction can be carried out under very mild conditions (weakly acidic medium at 60 °C) in an aqueous environment. Here, we report the reaction of 2-NPH·HCl for the determination of biotin in pharmaceutical products or food with nutrient function claims. For further improvement in detection specificity, LC–MS is also applied. As described by Saitoh and Gamoh [15], hydrazide derivatives of organic acids were successfully detected by LC–MS with electrospray ionization.

2. Experimental

2.1. Reagent solutions

2-NPH·HCl (Tokyo Kasei Kogyo, Tokyo, Japan) solutions (0.02 M) were prepared by dissolving the reagent in water. A EDC·HCl (Dojindo Laboratories, Kumamoto, Japan) solution (0.25 M) was prepared by dissolving the reagent in methanol. A fresh working solution of EDC was prepared daily, by mixing with an equal part of a solution of 2% pyridine in ethanol. A potassium hydroxide solution (15%, w/v) in water was also prepared. All the reagent solutions were stable for at least 3 months when kept below 5 °C. Biotin was commercially available from Wako Pure Chemicals (Osaka, Japan). All other chemicals were of analytical-reagent grade, and solvents were of HPLC quality. The ultra-pure water used for sample preparation was obtained from a Milli-Q purification system (Millipore, Bedford, MA, USA).

2.2. Samples

Samples used for the recovery tests were typical commercial foods with nutrient function claims. One food was in the form of a tablet containing seven kinds of vitamin such as vitamin B_1 (6 mg/tablet), vitamin B_2 (5 mg/tablet), vitamin B_6 (5 mg/tablet), vitamin B_{12} (5 mg/tablet), niacin (8 mg/tablet), pantothenic acid (12 mg), folic acid (0.2 mg/tablet), but not biotin. The other food was a drink containing vitamin C (1000 mg/250 mL) as a nutrient, but not biotin.

2.3. Sample preparation

Tablets were finely powdered, with an amount corresponding to 40–200 μg being accurately weighed and added to 10 mL of water. The solution was sonicated for 10 min and centrifuged for 5 min at 10,000 rpm, followed by further filtration using a membrane filter (0.2 μm; Dismic-25CS, Toyo Roshi Kaisha, Tokyo, Japan). The beverage was used without pretreatment or was diluted with water to contain between 4 and 20 μg/mL of biotin. A Sep-Pak Plus tC18ENV cartridge (Waters) was conditioned by successively passing methanol (5 mL), and 5 mM tetrabutylammmonium bromide (TBA) solution (5 mL). Five mL of the sample solution was mixed with 1 mL of 5 mM TBA solution and loaded in the pre-conditioned cartridge. The cartridges were then washed with 5 mL of 5 mM TBA solution to remove matrix interference and the analyte was then eluted with 2 mL of methanol. The eluant was transferred to a 2 mL volumetric flask and brought to exactly 2 mL with additional methanol.

A 100 μL aliquot of methanol eluant was added to a screw vial containing 200 μL of 250 mM EDC·HCl solution and 200 μL of 2% pyridine solution. After the addition of 200 μL of 20 mM NPH·HCl solution, the mixture was heated at 25 °C for 10 min. To remove the interfering materials, 100 μL of 15% potassium hydroxide solution was added, and a mixture thus obtained was further heated at 60 °C for 10 min and then cooled. The resulting hydrazide mixture was injected directly into the HPLC and LC–MS systems.

3. Instruments

3.1. HPLC apparatus and conditions

HPLC analyses were performed on an LC-10 series (Shimadzu, Kyoto, Japan) liquid chromatography system equipped with two LC-10ADvp pumps, an SPD-10AVvp spectrophotometric detector, an SPD-M10Avp photodiode array detector, and a SIL-10ADvp autosampler. Data processing was carried out with a Class-VP LC workstation. For the reversed-phase column, an L-column ODS (250 × 4.6 mm, I.D., 5 μm) (Chemical Evaluation and Research, Tokyo, Japan) and a TSK guardgel ODS-80Ts (15 × 3.2 mm, I.D.) (Toso, Tokyo, Japan) were used. The detection wavelength was set at 400 nm and the column temperature was maintained at 40 °C. The mobile phase was the mixture of 20 mM potassium dihydrogenphosphate (pH 4.5) and acetonitrile (75:25), with a flow rate of 1 mL/min. Injection volume was 10 μL.

3.2. LC–MS

LC–MS measurements were carried out with an LC-10 series liquid chromatography system, coupled to a LC–MS-2010 mass spectrometer, equipped with an electro spray ionization source (ESI) (Shimadzu, Kyoto, Japan).

For the LC–ESI^+-MS a split system 1/4 was used to introduce the effluent into the ES. The probe voltage was held at +1.5 kV and the cone voltage was set to 10 V. The block heater

temperature was 200 °C and CDL temperature was 250 °C. The nebulizing gas flow was 1.5 L/min and the pressure of drying gas was maintained at 0.2 mPa. Mass spectra were acquired by scanning from *m/z* 100 to 500 and data were processed using software. The separation was performed in a Capcell Pak C18 UG120 (250 × 2 mm, I.D.) (Shiseido, Tokyo, Japan) under chromatographic conditions of: 0.1 ml/min flow-rate, 1 μl sample injection volume and a mixture of methanol and 5 mM ammonium acetate (1:1) as the mobile phase.

4. Results and discussion

4.1. Examination of derivatization conditions

Due to the weak chromophoric properties of biotin, resulting in relatively poor sensitivity and selectivity of detection, pre-column derivatization methods have been developed with HPLC, using the reagent 2-nitrophenylhydrazine hydrochloride (2-NPH*HCl) for the derivatization of carboxylic groups.

The reaction conditions were investigated following the reported method [12,13] in order to ensure the maximum derivatization of biotin. The structures of biotin and NPH ester of biotin were shown in Fig. 1. The condition of HPLC by UV detection was investigated following the method reported for the acid hydrazides of fatty acids [12]. The effect of the EDC·HCl concentration on the peak area was investigated, and there was little difference in HPLC peak area at 400 nm of products formed for EDC concentrations between 150 and 400 mM; therefore 250 mM of EDC·HCl was selected because it fell in the middle of this range. Peak area was not much affected by concentrations of pyridine from 1 to 4% (v/v). We selected 2% as a medium value within this wide range. The relationship between the peak area of the acid hydrazides and the concentration of 2-NPH·HCl showed little change between 15 and 30 mM, but concentrations greater than 40 mM showed a decrease in peak area.

The temperature of derivatization can be an important factor in the optimization process rate [12]; however, we found little difference in peak area between 20 and 30 °C after 10 min reaction time and as long as 50 min (Fig. 2). A higher temperature (60 °C) decreased peak area by approximately 20%. The peak area for biotin became more consistent after 10 min at 20–30 °C, which suggested that the derivatization was completed after 10 min. Thus, derivatization could be carried out at a room temperature of approximately 25 °C. The derivatives of biotin standard solutions were stable for at least 10 days when kept below 5 °C. However, the sample solutions purified from tablets through cartridges were often unstable. For example, the peak area decreased to 80% if purified sample solutions

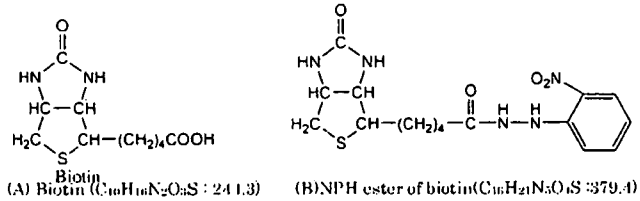

Fig. 1. Chemical structures of biotin (A) and NPH ester of biotin (B).

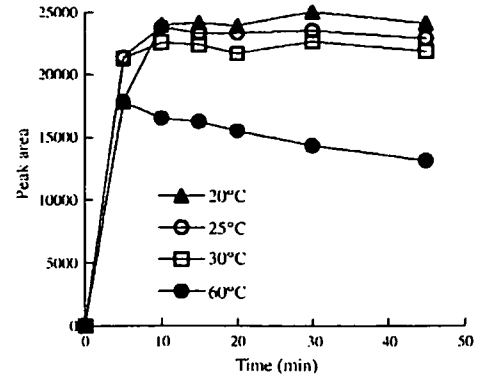

Fig. 2. Optimization of reaction time and reaction temperature for ester formation. A temperature of 25–50 °C had little effect on product formation between 10 and 50 min, whereas 60 °C reduced the total product formed by about 20%, and the reduction was greater with longer times.

stood for 3 h before derivatization. Therefore, the sample solutions should be converted immediately after preparation to the derivative.

4.2. HPLC separation and precision

Following the method described for the acid hydrazides of fatty acids [12], good chromatograms were obtained on reversed-phase columns using the mixture of 20 mM potassium dihydrogenphosphate (pH 4.5) and acetonitrile (75:25) as an eluent (Fig. 3A). The calibration curves were linear over the range 0.001–0.2 μg per injection (eight levels, three replicates, intercept; −691.56, slope; 41699, $r = 0.999$) and the relative standard deviation of peak areas of 0.06 μg per injection ($n = 6$) was 1.2%.

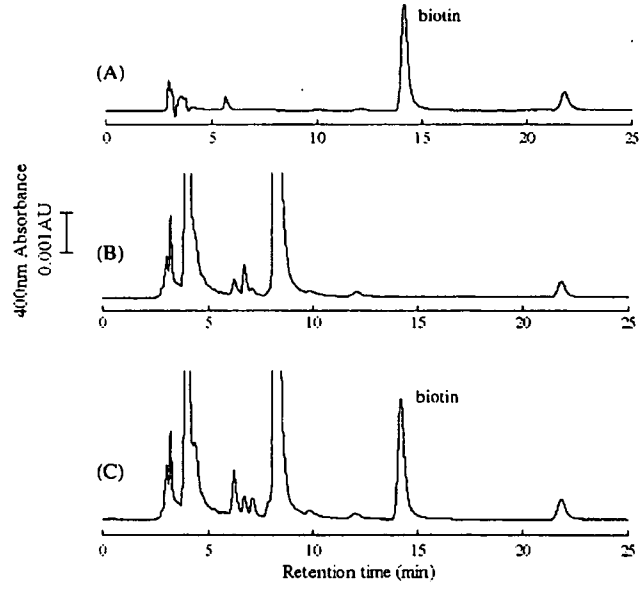

Fig. 3. HPLC chromatograms of tablet formulations: (A) standard solution of biotin NPH derivative (30 μg/mL), (B) tablet with no added biotin, (C) tablet with added biotin at 120 μg/tablet. Conditions: column, L-column (250 mm × 4.6 mm, I.D.); eluent, 20 mM potassium dihydrogenphosphate (pH 4.5) and acetonitrile (75:25); flow-rate, 1.0 mL/min; detection, UV at 400 nm; injection volume, 10 μL.

Table 1
Recovery tests of biotin with HPLC ($n = 6$)

	Amounts of added biotin	Recovery (%)
Standard solutions	5 μg/ml	97.7 ± 1.4
	50 μg/ml	103.2 ± 2.3
Products		
Tablet	120 μg/tablet	93.0 ± 1.7
Drink	5 μg/ml	73.3 ± 2.1

With HPLC, the detection limit was calculated to be 0.6 ng per injection ($S/N = 3$, $n = 6$), on the basis of S/N ratios.

4.3. Recovery test

Recovery testing was investigated using two products: a tablet and a drink, which contained several vitamins other than biotin. The results of recovery test were summarized in Table 1.

Satisfactory recoveries, ranging from 97.7 to 103.2%, were obtained when the whole procedure was performed at two levels of standard solutions, 5 and 50 μg/mL, respectively. The recoveries from the tablet, using HPLC after adding 120 μg biotin per tablet, are 93.0%. In the case of the drink, 73.3% was obtained when 5 μg of biotin was added per mL of the drink. HPLC chromatograms obtained for the recovery test from the tablet are shown in Fig. 3. Fig. 3A is the chromatogram for the standard solution of biotin NPH derivative and Fig. 3B is that for the tablet with no added biotin. As shown in Fig. 3C, the peaks for biotin were well separated from other large peaks and the peaks derived from the reagents were not distinctly observed. In many other derivatization methods such as fluorometric detection, there is a difficulty to spend too long analytical time to elute completely the large reagent peaks after a biotin peak. In this analytical procedure, other carboxylic vitamins, such as nicotinic acid, pantothenic acid and folic acid, were also detected as their derivatives. Their retention times in the same chromatographic conditions as Fig. 3C were confirmed by injecting each standard solution separately to be 12.7 min for nicotinic acid, 4 and 8 min for pantothenic acid, 4 and 4.4 min for folic acid. Folic acid may produce two derivatives due to its two carboxylic residues. However, in case of pantothenic acid, the reason for elution in two peaks was not clear. In Fig. 3B and C, the large peaks near 4 and 8 min may be derived from pantothenic acid contained in tablets.

The precision of the method was validated by both intra-day and inter-day variances in the case of the recoveries from the tablet. To determine intra-day variance, the assays were carried out five times in a day. Inter-day variance was determined by analyzing the samples over three days. From these results, the repeatability was 1. 5% and intermediate precision was 2.5%. The limit of quantification was 2 μg/mL as the initial sample solutions before the step of purification by Sep-Pak cartridges.

4.4. Confirmation test with LC–MS

In analyzing the sample solutions extracted from tablets by HPLC, sometimes the interference peak appeared near the biotin peak. Therefore, for a confirmation test, the MS detection was adopted. In the analysis of biotin derivatives by LC–MS, using ESI in both the positive and negative mode, a high sensitivity was achieved using the mobile phase of 5 mM ammonium acetate/methanol (1:1) solution. The positive and negative mass spectra of 2-NPH derivatives of biotin showed, not only molecular related ions ($[M + H]^+$ (m/z 380) and $[M - H]^-$ (m/z 378)), but also an m/z 418, potassium-loaded ion in positive mode. (Fig. 4A and B). The calibration curves of the selected ion monitoring (SIM) chromatograms of $[M + H]^+$ (m/z 380), were linear over the range 0.6–6 ng per injection (six levels, three replicates, intercept; 12097, slope; 19735, $r = 0.9996$) and the relative standard deviation of peak areas of 6 ng/injection ($n = 6$) and also 0.6 g per injection ($n = 6$) were less than 2%. The detection limit of biotin derivative in LC–MS was calculated to be 0.025 ng per injection ($S/N = 3$, $n = 6$). Applying the SIM chromatograms, acceptable recoveries of 97.5 ± 3.2% ($n = 6$) were obtained for tablets without any other peak. These results showed that 2-NPH derivatives of biotin can be well identified with ESI-MS detection.

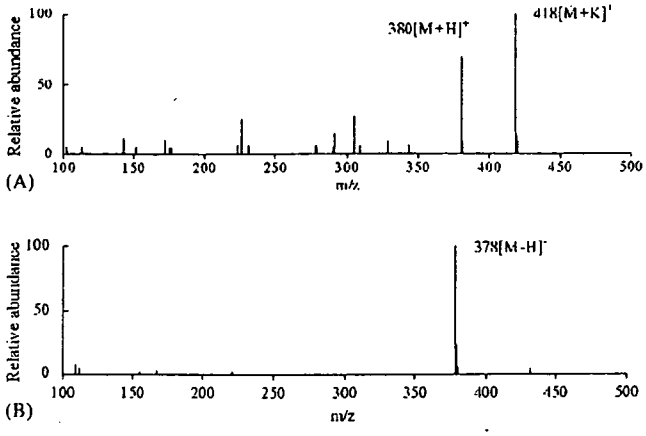

Fig. 4. LC–MS (ESI) spectra of NPH derivatives of biotin:(A) positive ion spectrum with molecular-related ions at m/z 380 and the potassium-loaded ion at m/z 418, (B) negative ion spectrum with the molecular-related ion at m/z 378.

5. Conclusion

Biotin can be selectively analyzed in an aqueous environment by derivatization with 2-NPH with UV-detection. Biotin derivatives can also be easily identified with LC–MS with ESI. From these results, this reaction appeared to be specific for the determination of as little as 0.6 ng of biotin, in the presence of large quantities of other substances. The proposed method could be used to specifically determine the presence of biotin in supplements and in pharmaceutical preparations.

References

[1] Japan Food Additives Association: Japan's Specifications and Standards for Food Additives, Tokyo, 2006.
[2] Analytical Methods for Food Additives in Food, Nihon Shokuhin Eisei Kyoukai, Tokyo, 2000, p. 230.
[3] E. Livaniou, D. Costopoulo, I. Vassiliadou, L. Leondiadis, J.O. Nyalala, D.S. Ithakissios, G.P. Evangelatos, J. Chromatogr. A 881 (2000) 331.

[4] P.L. Desbene, S. Coustal, F. Frappier, Anal. Biochem. 128 (1983) 359.
[5] Y. Kanazawa, T. Nakano, H. Tanaka, NIPPON KAGAKU KAISHI 3 (1984) 434.
[6] K. Hayakawa, J. Oizumi, J. Chromatogr. 413 (1987) 247.
[7] T. Yoshida, A. Uetake, C. Nakai, N. Nimura, T. Kinoshita, J. Choromatogr. 456 (1988) 421.
[8] K. Kamata, T. Hagiwara, M. Takahashi, S. Uehara, K. Nakayama, K. Akiyama, J. Chromatogr. 356 (1986) 326.
[9] M. Azoulay, P.L. Desbene, F. Frappier, J. Chromatogr. 303 (1984) 272.
[10] R. Wolf, C. Huschka, K. Raith, W. Wohlab, R. Neubert, Anal. Commun. 34 (1997) 355.
[11] U. Höller, F. Wachter, C. Wehrli, C. Fizet, J. Chromatogr. B 831 (2006) 8.
[12] H. Miwa, C. Hiyama, M. Yamamoto, J. Chromatogr. 321 (1985) 165.
[13] H. Miwa, J. Chromatogr. A 881 (2000) 365.
[14] R. Peters, J. Hellenband, Y. Mengerink, A. Ven der Wal, J. Chromatogr. A 1031 (2004) 35.
[15] H. Saitoh, K. Gamoh, BUNSEKI KAGAKU 52 (2003) 923.

Inhibition of Mannitol Crystallization in Frozen Solutions by Sodium Phosphates and Citrates

Ken-ichi IZUTSU,* Chikako YOMOTA, and Nobuo AOYAGI

National Institute of Health Sciences; 1–18–1 Kamiyoga, Setagaya-ku, Tokyo 158–8501, Japan.
Received November 10, 2006; accepted January 15, 2007; published online January 19, 2007

Effects of co-solutes on the physical property of mannitol and sorbitol in frozen solutions and freeze-dried solids were studied as a model of controlling component crystallinity in pharmaceutical formulations. A frozen mannitol solution (500 mM) showed a eutectic crystallization exotherm at −22.8 °C, whereas sorbitol remained amorphous in the freeze-concentrated fraction in the thermal scan. Various inorganic salts reduced the eutectic mannitol crystallization peak. Trisodium and tripotassium phosphates or citrates prevented the mannitol crystallization at much lower concentrations than other salts. They also raised transition temperatures of the frozen mannitol and sorbitol solutions (T_g': glass transition temperature of maximally freeze-concentrated amorphous phase). Crystallization of some salts (*e.g.*, NaCl) induced crystallization of mannitol at above certain salt concentration ratios. Thermal and near-infrared analyses of cooled-melt amorphous sorbitol solids indicated increased intermolecular hydrogen-bonding in the presence of trisodium phosphate. The sodium phosphates and citrates should prevent crystallization of mannitol in frozen solutions and freeze-dried solids by the intense hydrogen-bonding and reduced molecular mobility in the amorphous phase.

Key words amorphous; crystallization; formulation; freeze-drying; thermal analysis

Active ingredients and excipients in pharmaceutical solid formulations are in the amorphous or crystalline states. Application of amorphous solids is receiving increasing attention because of the unique physical and functional properties (*e.g.*, higher dissolution rate, stabilization of freeze-dried proteins).[1—4] Controlling the component crystallinity through optimizing the compositions and the manufacturing process (freeze-drying, quench cooling of hot-melt liquids) is a relevant method in formulation development because each ingredient and excipient possess different intrinsic propensity for crystallization.[5—7] Freeze-drying with a large amount of "inert" nonionic molecules (*e.g.*, disaccharides, soluble polymers) that are likely to form amorphous solid, is a popular way to obtain the intrinsically crystallizing ingredient in the non-crystalline dispersed state. The method, however, has some limitations in terms of the applicable excipients and the physical properties of the resulting solids.[8] Various inorganic salts also prevent crystallization of other solutes in frozen solutions and freeze-drying processes through mixing and/or complex formation.[9—11]

Mannitol is a popular excipient that tends to crystallize in frozen aqueous solutions.[12] The superior cake appearance and physical stability of the crystalline freeze-dried solids make mannitol a good bulking agent for many parenteral formulations of low-molecular-weight pharmaceutics. The crystallization process of mannitol in frozen solutions, the resulting crystal polymorphs, and the effect of co-solutes on the physical properties have been studied extensively as models to elucidate the component crystallization process in multi-solute systems.[13—19] Co-lyophilization with sucrose prevents crystallization of mannitol during freeze-drying at sucrose/mannitol weight concentration ratios above 2—3.[8,20,21] Some salts (*e.g.*, NaCl) that possess high melt miscibility with mannitol prevent its crystallization in frozen solutions at much lower concentrations than sucrose, whereas the low transition temperatures (T_g': glass transition temperature of the maximally freeze-concentrated amorphous phase) of the frozen solutions make it difficult to freeze-dry without physical collapse.[9,12,22]

Reduction of molecular mobility in the freeze-concentrated phase is another approach to obtain amorphous freeze-dried solids. Some salts (*e.g.*, sodium tetraborate, boric acid) that effectively raise T_g's of frozen polyol solutions (*e.g.*, saccharides, sugar alcohols) by complex formation would prevent spatial rearrangement of the mannitol molecules required for crystallization.[23—25] Recent studies showed that some pH-adjusting excipients (*e.g.*, sodium phosphate buffer) also raise glass transition temperature (T_g) of amorphous freeze-dried saccharides.[26,27] Some phosphate salts also prevent crystallization of mannitol during freeze-drying processes, suggesting contribution of the reduced molecular mobility in the amorphous mixture.[3,22,28] The purpose of this study was to elucidate the effect of phosphate and citrate salts on the physical properties of mannitol and sorbitol in the frozen aqueous solutions and in the dried solids. Different intrinsic tendency of mannitol and its isomer (sorbitol) for crystallization provided information on the mechanisms and requirements to obtain the stable amorphous solids. Controlling the component crystallinity by the widely used excipients should be of practical importance in developing formulations without particular safety concerns.

Experimental

Materials All the proteins and other chemicals employed in this study were of analytical grade and obtained from the following commercial sources: sucrose (Sigma-Aldrich, St. Louis, MO, U.S.A.); trisodium phosphate·12H_2O (Katayama Chemical, Osaka, Japan); disodium hydrogen citrate and sodium dihydrogen citrate (Kanto Chemical, Tokyo, Japan); D(+)-mannitol, D-sorbitol, and other chemicals (Wako Pure Chemical, Osaka).

Freeze-Drying and Preparation of Amorphous Solids Aqueous solutions (250 μl) containing 500 mM mannitol and various concentrations of co-solutes in flat-bottom glass vials (10 mm diameter) were lyophilized using a freeze-drier (Freezevac 1C; Tozai Tsusho, Tokyo). The solutions were frozen by immersion in liquid nitrogen, transferred to the shelf of the freeze-dryer, and lyophilized without a shelf temperature control for 12 h and at 35 °C for 4 h. The solids were applied for the thermal analysis within 48 h of the preparation. Mixed powders containing sorbitol (approx. 200 mg), salt, and

* To whom correspondence should be addressed. e-mail: lzutsu@nihs.go.jp

aliquot of water (50 μl) in crystal cuvettes or glass tubes were heated under vacuum at 160 °C for 20 min using a drying oven (DP23, Yamato Scientific Inc., Tokyo), then cooled at room temperature to prepare amorphous solids for thermal and spectroscopic analyses.

Thermal Analysis Thermal analyses of frozen solutions and freeze-dried solids were performed using a differential scanning calorimeter (DSC-Q10; TA Instruments, New Castle, DE, U.S.A.) with an electric refrigerating system and associated software (Universal Analysis). Indium and cyclohexane were used for the DSC calibration. Aliquots of solutions (10 μl) in aluminum cells were scanned from −70 °C at 5 °C/min after the system had been cooled at −10 °C/min to study the thermal profile of the frozen solutions. The effect of a heat treatment (annealing) on the thermal properties of the frozen solutions was studied after the initial heating scan was paused at −10 °C, and then the samples were maintained at the temperature for 30 min. Thermal data were acquired in the subsequent heating scan from −70 °C at 5 °C/min. The extent of mannitol crystallization exotherm was obtained from the peak area under the baseline of the heat flow. Peaks in the derivative thermograms were assigned to glass transition temperatures of the maximally freeze-concentrated amorphous phases (T'_gs). Thermal analyses of the freeze-dried solids (1.7—2.2 mg) were performed from −30 °C at 10 °C/min. The cooled-melt solids (approx. 5 mg) were scanned from −30 °C at 5 °C/min.

Near-Infrared Spectroscopy Near-infrared analysis was performed using a FT-NIR system (MPA, Bruker Optik GmbH, Germany) with OPUS software. Absorbance of the sample (1-mm light path length) at 4000 to 12000 cm^{-1} range was obtained at room temperature (25 °C) with a 2 cm^{-1} resolution in 128 scans.

Results

Figure 1 shows thermograms of frozen solutions containing an identical concentration (500 mM) of various solutes. Frozen citric acid and sodium citrate solutions showed thermograms typical for amorphous supercooled freeze-concentrated phase, with the baseline shifts (T'_g) at −53.4 °C (citric acid), −33.4 °C (sodium dihydrogen citrate), −38.8 °C (disodium hydrogen citrate), and −42.5 °C (trisodium citrate).[29] The transitions (T'_gs) of frozen sucrose and sorbitol solutions were observed at −33.8 °C and −44.2 °C, respectively. Some other frozen solutions (500 mM H_3PO_4, NaH_2PO_4, K_3PO_4, LiCl) showed a gradual shift of the thermogram baseline that suggested an amorphous freeze-concentrated phase with T'_g below −55 °C. Freezing of aqueous solutions containing di- and trisodium phosphate (Na_2HPO_4, Na_3PO_4) solutions showed endotherm peaks in the cooling process (data not shown) and flat thermograms in the heating scan, indicating that the salt crystallization was completed before the heating scan.[5,30] Some frozen salt solutions showed endotherm peaks that indicated eutectic crystal melting at −19.8 °C (NaCl), −8.9 °C (KCl), and −14.2 °C (RbCl) (data not shown). The peak temperatures were slightly (approx. 2 °C) higher than the values in some literature probably because of the higher scanning rate in this study.[5,6,31]

Figure 2 shows DSC scans of frozen solutions containing 500 mM mannitol (approx. 91.1 mg/ml) and varied concentrations of sodium hydrogen phosphates (Na_2HPO_4, NaH_2PO_4, Na_3PO_4) in the first heating scan from −70 °C, and in the second heating scan after a heat treatment (annealing) at −10 °C for 30 min. The frozen mannitol solution showed a large eutectic crystallization exotherm peak at −22.8 °C in the first scan. Several smaller thermal events, including two possible T'_gs (T'_{g1}: −37.5 °C, T'_{g2}: −29.0 °C) and a small endotherm (−24.3 °C), were also observed prior to the crystallization exotherm.[17,21,28] A small exotherm peak that suggests partial crystallization was observed in the cooling process of some frozen mannitol solutions (data not shown). The second scan of the frozen mannitol solution after the

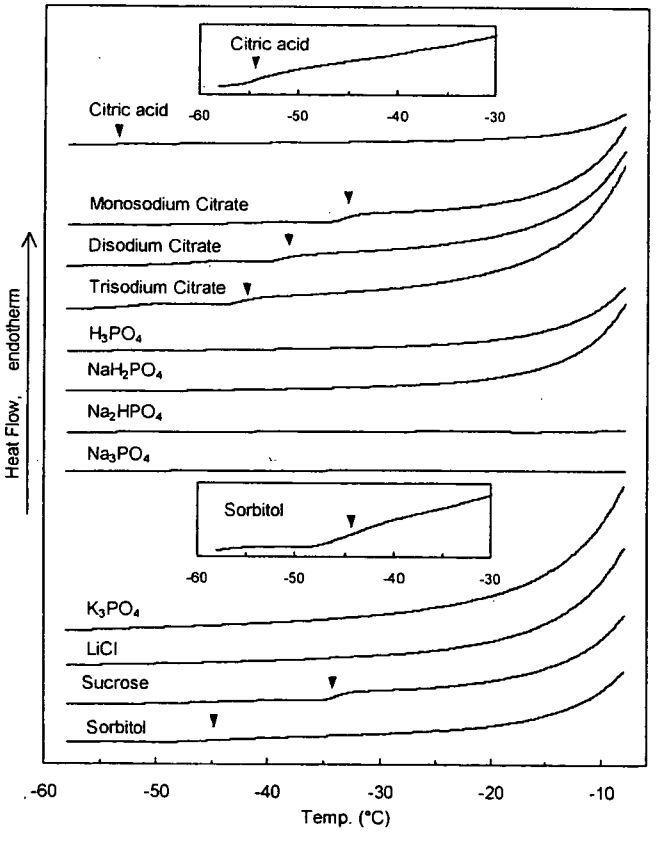

Fig. 1. Thermal Profiles of Frozen Single-Solute Aqueous Solutions (500 mM, 10 μl) Scanned from −70 °C at 5 °C/min

Glass transition temperatures of the maximally freeze-concentrated amorphous phases (T'_gs) are marked with reversed triangles (▼).

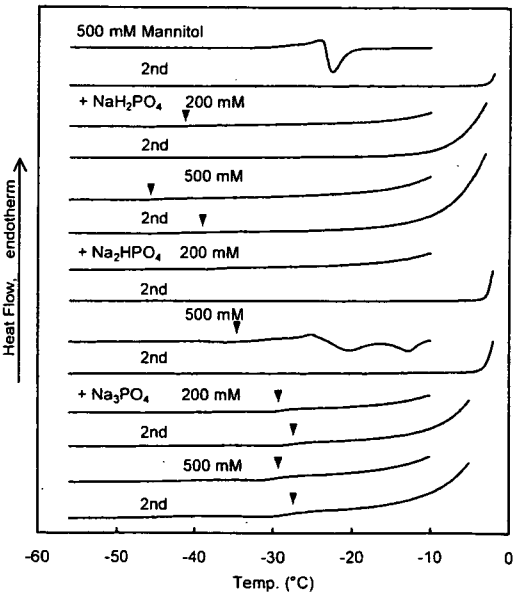

Fig. 2. Thermal Profiles of Frozen Solutions Containing Mannitol (500 mM) and Varied Concentrations of Sodium Phosphates in the First Scan from −70 °C at 5 °C/min (Upper) and the Second Scan after a Heat Treatment at −10 °C for 30 min

The glass transitions (T'_gs) are marked with reversed triangles (▼).

heat treatment resulted in a flat thermogram up to the ice-melting temperature, indicating the crystallized mannitol in the frozen solution.

The phosphate salts showed varied effects on the thermal property of the frozen mannitol solution. The mannitol crystallization exotherm peak disappeared in the presence of NaH_2PO_4 (200, 500 mM), Na_2HPO_4 (200 mM) or Na_3PO_4 (200, 500 mM), presenting a thermal transition (T'_g) that indicated the amorphous freeze-concentrated phase surrounding ice crystals. The frozen solution containing 500 mM mannitol and 500 mM Na_2HPO_4 showed two exotherm peaks that suggest crystallization of mannitol (−20.3 °C) and Na_2HPO_4 (−12.8 °C). The second scan of frozen solutions containing mannitol and NaH_2PO_4 (500 mM) or Na_3PO_4 (200, 500 mM) also showed the T'_g transitions. A slight shift of the transition temperature (T'_g) in the second scan suggested retention of the amorphous freeze-concentrated phase and some re-ordering (*e.g.*, further ice crystal growth) of the frozen solution during the heat treatment.[17] The second scan of frozen solutions containing mannitol and Na_2HPO_4 (200, 500 mM) showed flat thermograms up to the ice-melting temperature, indicating the crystallized mannitol and the salt.[18]

Figures 3 and 4 show effects of various co-solutes (*e.g.*, phosphate, citrate, chloride salts) on the mannitol crystallization exotherm size and transition temperatures (T'_gs) of the frozen solutions. The crystallization exotherm of the frozen mannitol solution (500 mM) was 14.1±1.2 J/g (n=3). Most of the solutes, except H_3PO_4, apparently reduced the mannitol crystallization peak concomitantly with the upward shift of the peak temperature. Alkali-metal chloride salts with smaller cations (LiCl, NaCl) were more effective at reducing the mannitol crystallization peak than those with larger cations (KCl, RbCl). The mannitol crystallization peak also disappeared in the presence of 200 mM sucrose or 150 mM CH_3COONa, indicating the prominent effect of the salts, especially compared in their weight concentrations. Addition of some solutes slightly increased the exotherm at lower concentrations (<100 mM), probably because they alter thermal transitions prior to the crystallization peak. Sodium and potassium phosphates showed varied ability to reduce the mannitol crystallization peak depending on the ionic valencies. The mannitol crystallization peak disappeared at different phosphate salt concentrations (Na_3PO_4, K_3PO_4<Na_2HPO_4, K_2HPO_4<NaH_2PO_4<KH_2PO_4). Sodium phosphate buffers containing both NaH_2PO_4 and Na_2HPO_4 at different concentration ratios (3 : 1, 1 : 1, and 1 : 3) showed the crystallization-preventing effects intermediate between those of the individual salt solutions (data not shown). The mannitol crystallization peak also disappeared at different sodium citrate and citric acid concentrations (trisodium citrate<disodium citrate<monosodium citrate<citric acid). The pronounced effect of tri- and divalent salts suggests the significance of ion concentrations or alkaline pH on the ability of co-solutes to prevent the mannitol crystallization. The mannitol crystallization peak re-appeared upon further addition of some salts (300—500 mM Na_2HPO_4, 500 mM RbCl,

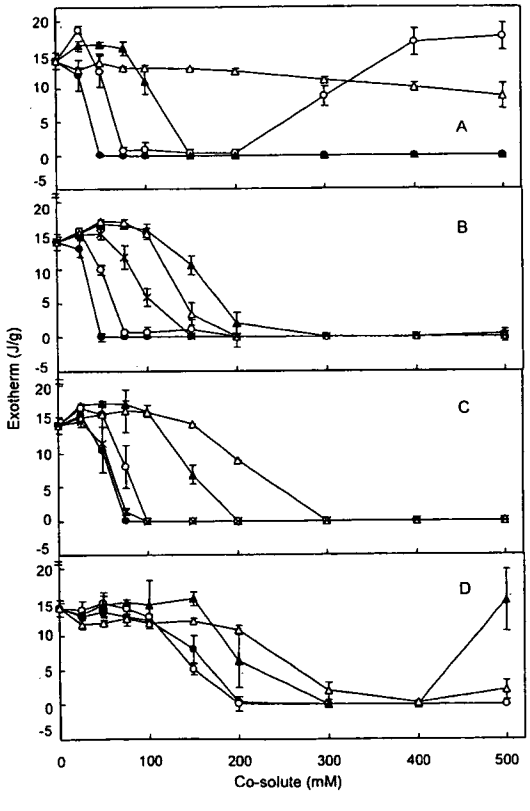

Fig. 3. Effects of Co-solutes on the Mannitol Crystallization Exotherm in Frozen Aqueous Solutions (10 μl) Scanned from −70 °C at 5 °C/min

The symbols denote frozen solutions containing (A) ●: Na_3PO_4, ○: Na_2HPO_4, ▲: NaH_2PO_4, △: H_3PO_4, (B) ●: K_3PO_4, ○: K_2HPO_4, ▲: KH_2PO_4, △: sucrose, ×: CH_3COONa, (C) ●: trisodium citrate, ○: disodium citrate, ▲: monosodium citrate, △: citric acid, ×: tripotassium citrate, (D) ●: LiCl, ○: NaCl, ▲: KCl, △: RbCl (mean value±S.D., n=3).

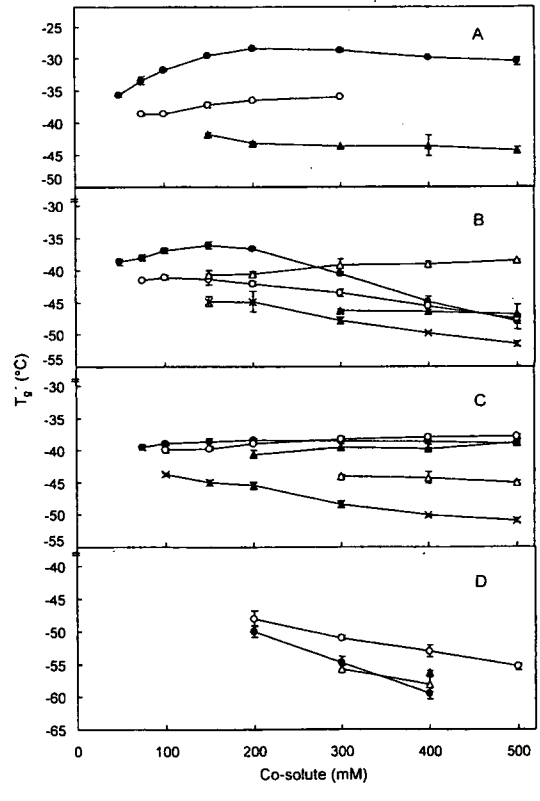

Fig. 4. Thermal Transition Temperatures (T'_g: Glass Transition of the Maximally Freeze-Concentrated Amorphous Phases) of the Frozen Solutions (10 μl) Containing Mannitol (500 mM) and Various Concentrations of Co-solutes Scanned from −70 °C at 5 °C/min

Symbols denote the co-solutes shown in Fig. 3 (mean value±S.D., n=3).

500 mM KCl). Crystallization of these salts in the single-solute frozen solutions (Fig. 1) suggested that the salt crystallization at high salt/mannitol ratio induced the mannitol crystallization in the remaining phase.

Frozen solutions containing the amorphous state mannitol and co-solute combinations showed apparent T'_g transition (Fig. 4). Extrapolating the transition temperatures of these mixture solutions suggested that T'_g of the frozen single-solute mannitol solution occurred at approximately −40 °C, which should correspond to the reported lower-temperature transition (T'_{g1}).[21,28] Addition of some salts (*e.g.*, NaH_2PO_4, CH_3COONa, LiCl, NaCl, KCl, RbCl) lowered the transition temperature linearly depending on their concentrations. Sucrose slightly shifted the transition toward its intrinsic T'_g (−33.8 °C, Fig. 1).[21] These findings suggest simple mixing of the solutes in the freeze-concentrated phase, which transition temperature depends on the T'_gs of the individual components and their concentration ratios. In contrast, some phosphate and citrate salts non-linearly raised the transition temperature. Frozen solutions containing mannitol and trisodium or tripotassium salts (Na_3PO_4, K_3PO_4, trisodium citrate) showed the highest transition temperatures at certain (150—300 mM) co-solute concentrations. The transition temperatures above those of the individual solutes (*e.g.*, trisodium citrate: −42.5 °C) suggested reduced molecular mobility in the freeze-concentrated phase.

Sorbitol remained amorphous in the single-solute (500 mM) frozen solution, presenting a T'_g transition at −44.2 °C (Fig. 1). Effect of the salts on the transition temperature of the frozen sorbitol solution (T'_g, Fig. 5) showed similar trends with the mannitol-salt systems. The non-linear upward shift of T'_gs suggested some interaction between the Na_3PO_4 and the sugar alcohols, or altered environment in the freeze-concentrated phase. A salt crystallization exotherm peak was observed in the solutions containing 500 mM sorbitol and 300—500 mM Na_2HPO_4. Addition of 500 mM Na_2HPO_4 resulted in low T'_g (−45.0 °C) that suggested transition of phase-separated sorbitol fraction.

Effects of sodium phosphates and citrates on the physical properties of freeze-dried mannitol was studied (Fig. 6). Freeze-drying of mannitol resulted in α or β polymorph crystal that showed a large crystal melting endotherm at approximately 170 °C.[18,32] Co-lyophilization with the phosphate and citrate salts resulted in the small crystal melting peaks that suggested lower crystallinity or different polymorph (*e.g.*, δ-form) in the solid.[9,18,32] Some solids showed glass transitions (35—55 °C), exotherm peaks of putative mannitol crystallization (60—80 °C), and small mannitol crystal melting peaks (150—170 °C). Transition temperatures (T_gs) of these co-lyophilized solids were higher than the reported T_g of amorphous mannitol (approx. 13 °C).[33] Freeze-dried solids containing mannitol and trisodium phosphate or citrate showed T_gs (52.9, 43.7 °C) higher than those of the corresponding disodium salts (44.5, 40.0 °C). Co-lyophilization with a higher concentration (200 mM<) of the co-solutes further reduced the mannitol crystallization during the process (data not shown). The upper shift of the glass transition temperature (T_g) suggested altered interaction (*e.g.*, hydrogen-bonding) between mannitol molecules, as was reported in co-lyophilization of disaccharides with the phosphate salts.[26]

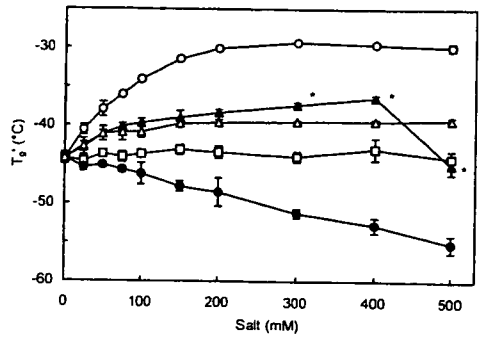

Fig. 5. Effect of Co-solutes on T'_g of Frozen Sorbitol (500 mM) Solutions

An aliquot of solution (10 μl) in aluminum cell was scanned from −70 °C at 5 °C/min. Symbols represent measured midpoint values±S.D. (n=3, ○: Na_3PO_4, ▲: Na_2HPO_4, △: trisodium citrate, □: NaH_2PO_4, ●: NaCl).

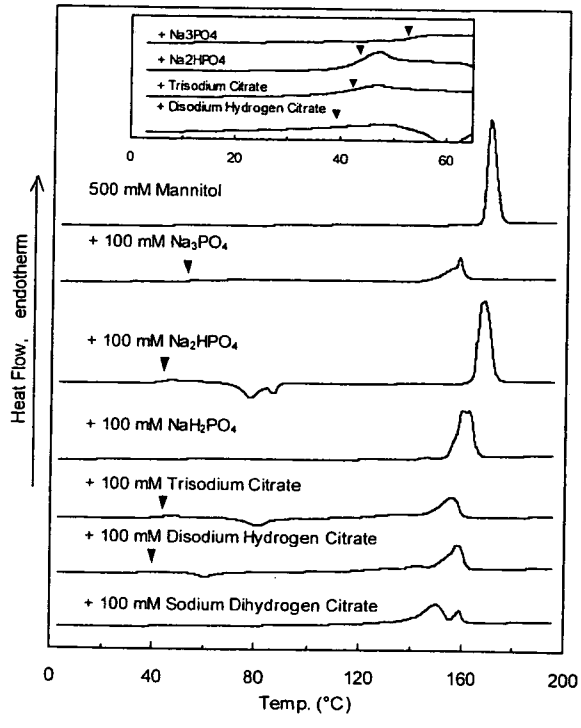

Fig. 6. Thermal Profiles of Freeze-Dried Solids Obtained from Initial Solutions Containing Mannitol (500 mM) and Various Co-solutes (100 mM)

Some thermograms were magnified to indicate the glass transition temperatures of the solids (▼).

Thermal and near-infrared analyses of cooled-melt amorphous sorbitol solids were performed to study the possible salt-induced changes in molecular interactions. A thermogram of cooled-melt sorbitol solid, and effects of the salts on the glass transition temperature (T_g: −1.1 °C) are shown in Fig. 7. The amorphous sorbitol solid showed only a glass transition in the thermal scan up to 125 °C. Trisodium phosphate and citrate exhibited much larger effect to raise the T_g of the amorphous sorbitol solid than Na_2HPO_4 and NaCl, suggesting significant reduction in the molecular mobility. Near-infrared spectra of the cooled-melt amorphous sorbitol solid showed several broad bands that indicate random molecular configurations (Fig. 8). The bands in the 6000 to 7000 cm^{-1} range have been assigned as O–H stretch first overtones of hydroxyl groups with intermolecular (around 6350 cm^{-1}) and intramolecular (around 6800 cm^{-1}) hydro-

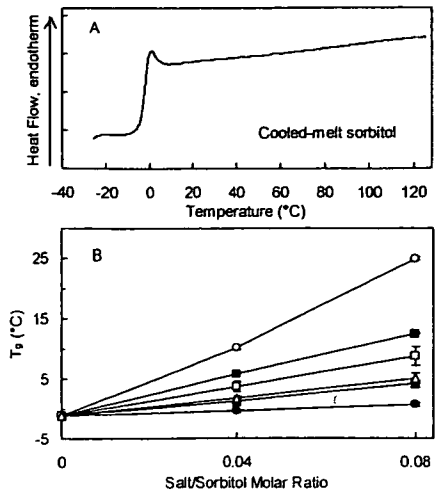

Fig. 7. Thermal Profile (A) and Glass Transition Temperatures (B) of Cooled-Melt Sorbitol–Salt Mixture Solids

Symbols represent measured midpoint T_g values±S.D. (n=3, ○: Na_3PO_4, ▲: Na_2HPO_4, ■: trisodium citrate, □: disodium citrate, △: monosodium citrate, ●: NaCl).

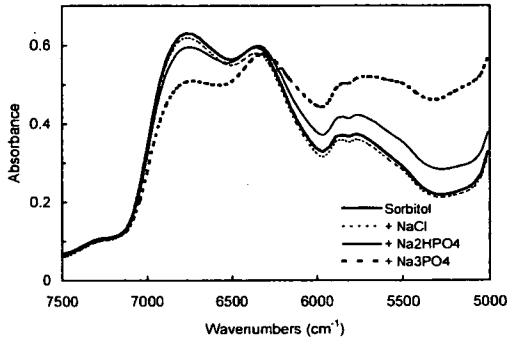

Fig. 8. Transmission Near-Infrared Spectra of Cooled-Melt Solids Containing Sorbitol and Salts (Na_3PO_4, Na_2HPO_4, NaCl) in the Molar Ratio of 12.5 : 1

gen-bonding.[34,35] Addition of Na_3PO_4 reduced intensity of the band at 6800 cm^{-1} with concomitant increase in the bands below 6350 cm^{-1}, suggesting increased intermolecular hydrogen-bonding in the solid. The intense molecular interaction should result in the higher transition temperatures. Absorbance by the phosphate salts should also contribute to the increased intensity in the lower wavenumber region (5500—6000 cm^{-1}).[34,35] Partial crystallization of cooled-melt mannitol made the solid inappropriate for the NIR study.

Discussions

Various co-solutes, including popular excipients in pharmaceutical formulations, kinetically and/or thermodynamically prevented the crystallization of mannitol in frozen solutions at certain concentrations. Trisodium and tripotassium phosphates or citrates showed larger effect to prevent the mannitol crystallization in the frozen solutions and freeze-dried solids. The sorbitol and salt combinations indicated reduced mobility of molecules by intense hydrogen-bonding in the freeze-concentrated phase, which should contribute to retain mannitol in the amorphous state.

Miscibility of mannitol and co-solutes in the concentrated fraction should be the first requisite to prevent the mannitol crystallization in frozen solutions. Mannitol and the various co-solutes were freeze-concentrated into the same phase at certain concentration ratios, and under this condition mixing should kinetically perturb the spatial rearrangement of mannitol molecules required for crystallization. Reported significant melt miscibility of mannitol and some salts (*e.g.*, NaCl) at elevated temperatures suggested their thermodynamic compatibility in the concentrated mixture phase in frozen solutions.[9] On the other hand, thermodynamic solute immiscibility and/or co-solute crystallization (*e.g.*, Na_2HPO_4) at above their critical mixing co-solute/mannitol concentration ratios should separate the solutes to different phases in a frozen solution.[36] The co-solute crystallization should induce crystallization of the remaining mannitol molecules. Various factors, including the structure, ionized state and concentrations of co-solutes, as well as the thermal process, should determine the miscibility with mannitol in the frozen solutions.

Reduction of the molecular mobility of mannitol should be another significant requirement to prevent its crystallization in frozen solutions. The upward shift of the transition temperatures (T_g's) in the presence of some phosphate and citrate salts should indicate the reduced molecular mobility in the freeze-concentrated phases. Some of the combinations showed their highest T_g's at certain salt concentrations, which suggested direct interaction between mannitol and co-solute ions and/or altered molecular interactions between mannitol molecules rather than simple mixing.[23,24] It is plausible that the salt-induced intense intermolecular hydrogen-bonding observed in the cooled-melt sorbitol system also contributes to prevent mannitol crystallization in frozen solution and freeze-dried solids. The different effects of phosphate and citrate salts suggested that ionic valence and local pH are the significant factors involved in altering the molecular interactions. The effect of pH on the molecular interaction between polyols are subject to debate, and will require further study.[26,37]

References

1) Hancock B. C., Zografi G., *J. Pharm. Sci.*, **86**, 1—12 (1997).
2) Craig D. Q., Royall P. G., Kett V. L., Hopton M. L., *Int. J. Pharm.*, **179**, 179—207 (1999).
3) Izutsu K., Yoshioka S., Terao T., *Chem. Pharm. Bull.*, **42**, 5—8 (1994).
4) Pikal M. J., Dellerman K. M., Roy M. L., Riggin R. M., *Pharm. Res.*, **8**, 427—436 (1991).
5) Chang B. S., Randall C., *Cryobiology*, **29**, 632—656 (1992).
6) MacKenzie A. P., *Phil. Trans. R. Soc. Lond. B.*, **278**, 167—189 (1971).
7) Suzuki T., Franks F., *J. Chem. Soc., Faraday Trans.*, **89**, 3283—3288 (1993).
8) Kim A. I., Akers M. J., Nail S. L., *J. Pharm. Sci.*, **87**, 931—935 (1998).
9) Telang C., Suryanarayanan R., Yu L., *Pharm. Res.*, **20**, 1939—1945 (2003).
10) Tong P., Taylor L. S., Zografi G., *Pharm. Res.*, **19**, 649—654 (2002).
11) Izutsu K., Fujimaki Y., Kuwabara A., Aoyagi N., *Int. J. Pharm.*, **301**, 161—169 (2005).
12) Nail S. L., Jiang S., Chongprasert S., Knopp S. A., *Pharm. Biotechnol.*, **14**, 281—360 (2002).
13) Cannon A. J., Trappler E. H., *PDA J. Pharm. Sci. Technol.*, **54**, 13—22 (2000).
14) Yu L., Milton N., Groleau E. G., Mishra D. S., Vansickle R. E., *J. Pharm. Sci.*, **88**, 196—198 (1999).
15) Lu Q., Zografi G., *Pharm. Res.*, **15**, 1202—1206 (1998).
16) Williams N. A., Guglielmo J., *J. Parenter. Sci. Technol.*, **47**, 119—123 (1993).
17) Pyne A., Surana R., Suryanarayanan R., *Pharm. Res.*, **19**, 901—908

(2002).
18) Kett V. L., Fitzpatrick S., Cooper B., Craig D. Q., *J. Pharm. Sci.*, **92**, 1919—1929 (2003).
19) Martini A., Kume S., Crivellente M., Artico R., *PDA J. Pharm. Sci. Technol.*, **51**, 62—67 (1997).
20) Johnson R. E., Kirchhoff C. F., Gaud H. T., *J. Pharm. Sci.*, **91**, 914—922 (2002).
21) Lueckel B., Bodmer D., Helk B., Leuenberger H., *Pharm. Dev. Technol.*, **3**, 325—336 (1998).
22) Telang C., Yu L., Suryanarayanan R., *Pharm. Res.*, **20**, 660—667 (2003).
23) Miller D. P., Anderson R. E., de Pablo J. J., *Pharm. Res.*, **15**, 1215—1221 (1998).
24) Izutsu K., Ocheda S. O., Aoyagi N., Kojima S., *Int. J. Pharm.*, **273**, 85—93 (2004).
25) Yoshinari T., Forbes R. T., York P., Kawashima Y., *Int. J. Pharm.*, **258**, 109—120 (2003).
26) Ohtake S., Schebor C., Palecek S. P., de Pablo J. J., *Pharm Res.*, **21**, 1615—1621 (2004).
27) Kets E. P. W., IJpelaar P. J., Hoekstra F. A., Vromans H., *Cryobiology*, **48**, 46—54 (2004).
28) Cavatur R. K., Vemuri N. M., Pyne A., Chrzan Z., Toledo-Velasquez D., Suryanarayanan R., *Pharm. Res.*, **19**, 894—900 (2002).
29) Lu Q., Zografi G., *J. Pharm. Sci.*, **86**, 1374—1378 (1997).
30) Murase N., Franks F., *Biophys. Chem.*, **34**, 293—300 (1989).
31) Deluca P., Lachman L., *J. Pharm. Sci.*, **54**, 617—624 (1965).
32) Burger A., Henck J. O., Hetz S., Rollinger J. M., Weissnicht A. A., Stottner H., *J. Pharm. Sci.*, **89**, 457—469 (2000).
33) Yu L., Mishra D. S., Rigsbee D. R., *J. Pharm. Sci.*, **87**, 774—777 (1998).
34) Ozaki Y., Kawata S., "Near-Infrared Spectroscopy," Japan Scientific Societies Press, Tokyo, 1996.
35) Shenk J. S., Workman J. J., Jr., Westerhaus M. O., "Handbook of Near-Infrared Analysis," ed. by Burns D. A., Ciurczak W. W., Taylor & Francis, New York, 2001, pp. 419—474.
36) Randolph T. W., *J. Pharm. Sci.*, **86**, 1198—1203 (1997).
37) Eriksson J. H., Hinrichs W. L., de Jong G. J., Somsen G. W., Frijlink H. W., *Pharm. Res.*, **20**, 1437—1443 (2003).

Food Additives and Contaminants, August 2007; 24(8): 799–806

Taylor & Francis
Taylor & Francis Group

Quantitative nuclear magnetic resonance spectroscopic determination of the oxyethylene group content of polysorbates

NAOKI SUGIMOTO[1], RYO KOIKE[2], NORIKO FURUSHO[1], MAKOTO TANNO[2], CHIKAKO YOMOTA[1], KYOKO SATO[1], TAKESHI YAMAZAKI[1], & KENICHI TANAMOTO[1]

[1]*National Institute of Health Sciences: 1-18-1, Kamiyoga, Setagaya, Tokyo 158-8501, Japan and* [2]*Kao Corporation, Analytical Research Center, 1334, Minato, Wakayama-shi, Wakayama 640-8580, Japan*

(Received 30 November 2006; revised 5 February 2007; accepted 13 February 2007)

Abstract
Guidelines for the oxyethylene group (EO) content of polysorbates are set by the Food and Agriculture Organization/World Health Organization Joint Expert Committee on Food Additives. However, the classical titration method for EO determination is difficult and time-consuming. Here, we show that quantitative ^{1}H-nuclear magnetic resonance spectroscopy can determine the EO contents of polysorbates rapidly and simply. The EO signals were identified through comparisons with sorbitan monolaurate and poly(ethylene glycol) distearate. Potassium hydrogen phthalate was used as an internal standard. The EO contents were estimated from the ratio of the signal intensities of EO to the internal standard. Two nuclear magnetic resonance systems were used to validate the proposed method. The EO content of commercial polysorbates 20, 60, 65, and 80 was determined to be within the recommended limits using this technique. Our approach thus represents an additional or alternative method of determining the EO contents of polysorbates.

Keywords: *Analytical method, food additive, oxyethylene, polysorbate, quantitative nuclear magnetic resonance*

Introduction

Polysorbates are non-ionic surfactants that are widely used as emulsifiers, dispersants, and stabilizers in food processing. Polysorbates consist of a mixture of fatty-acid partial esters of sorbitol and condensed sorbitol anhydrides, and contain approximately 20 moles of ethylene oxide (comprising the oxyethlene unit [EO] $-OC_2H_4-$) for each mole of sorbitol, along with its monohydrides and dianhydrides. The main fatty acids of polysorbates 20, 60, 65, and 80 are monolauric acid, monostearic acid, tristearic acid, and monooleic acid, respectively. The typical structures of these polysorbates are shown in Figure 1.

Guidelines for the EO contents of polysorbates are set by the Food and Agriculture Organization (FAO)/World Health Organization (WHO) Joint Expert Committee on Food Additives (JECFA). To comply with the JECFA standards, the quality and composition of commercially synthesized polysorbates must be monitored and regulated. The standard method of measuring EO as described in "section VI. Methods for fats and related substances in the guide to specification" is as follows: "The oxyethylene groups are converted to ethylene and ethyl iodide which can be determined by titration. By utilizing a conversion factor determined on a reference sample, it is possible to compute the polyoxyethylene ester content" (JECFA [internet]). However, this classical titration method requires a complicated apparatus and involves several time-consuming steps. Alternative methods for determining the EO contents of polysorbates have not previously been reported, because these complex compounds are mixtures of isomers that are non-selectively substituted with EOs and fatty acids.

The quantitative nuclear magnetic resonance (qNMR) approach is based upon the International

Correspondence: Naoki Sugimoto. E-mail: nsugimot@nihs.go.jp

ISSN 0265-203X print/ISSN 1464-5122 online
DOI: 10.1080/02652030701278347

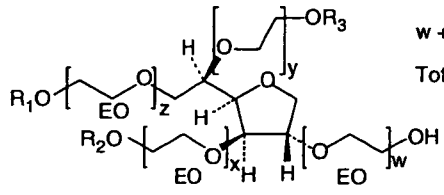

w + x + y + z = approx. 20

Total EO = (C_2H_4O) x (w + x + y + z) = $C_{40}H_{80}O_{20}$ (MW 881.1)

Compound			Formula (MW)	EO(%) in molecule
Polysorbate 20 (polyoxyethylene (20) sorbitan monolaurate)	R_1= 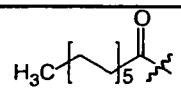	$R_2 = R_3 = H$	$C_{58}H_{114}O_{26}$ (MW1227.5)	EO(%) = 71.8
Polysorbate 60 (polyoxyethylene (20) sorbitan monostearate)	R_1= 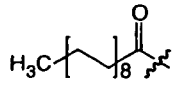	$R_2 = R_3 = H$	$C_{64}H_{126}O_{26}$ (MW1311.7)	EO(%) = 67.2
Polysorbate 65 (polyoxyethylene (20) sorbitan tristearate)	$R_1 = R_2 = R_3$ = 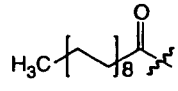		$C_{100}H_{194}O_{28}$ (MW1844.6)	EO(%) = 47.8
Polysorbate 80 (polyoxyethylene (20) sorbitan monooleate)	R_1= 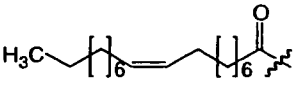	$R_2 = R_3 = H$	$C_{63}H_{122}O_{26}$ (MW1295.6)	EO(%) = 68.0

Figure 1. Typical structures of polysorbates 20, 60, 65, and 80. The formulae and EO (%) were estimated based on the assumption that there were 20 moles of EO per molecule.

system of units (SI units). This valuable technique meets the requirements of a primary ratio analytical method (Jancke 1998). The use of qNMR to determine the ethanol content of deuterium oxide solution was previously reported as a part of an intercomparison study organized by the Comité Consultatif pour la Quantité de Matère (CCQM). The results showed that the accuracy of qNMR was equivalent to that of gas chromatography with a flame ionization detector (GC-FID) (Saito et al. 2003). qNMR exploits the fact that the signal intensities of a given NMR resonance are directly proportional to the molar amount of the nucleus within the sample. qNMR can determine the quantity of a compound, its substituent contents, or its absolute quality if the whole sample weight is known. This technique has several advantages for the analysis of organic compounds: it is non-destructive, it provides both quantitative data and structural information about a compound, and high-throughput spectral-acquisition instruments are commercially available. The main drawback of the qNMR approach is that manual spectral assignment is required; however, this can easily be rectified by applying current NMR technical experiments such as total correlated spectroscopy (TOCSY), heteronuclear multiple quantum correlation (HMQC), heteronuclear multiple bond coherence (HMBC), etc.

Based on these features of qNMR, we predicted that the method could be used to determine the EO contents of polysorbates. In the current paper, we detail the application of qNMR along with an internal standard for the direct determination of the EO contents of polysorbates.

Materials and methods

Materials

Samples of reagent-grade polysorbates 20, 60, 65, 80, and sorbitan monolaurate (Span 20) were purchased from Wako Pure Chemical Industries, Ltd (Osaka, Japan). Poly(ethylene glycol) distearate was purchased from Sigma-Aldrich Japan KK (Tokyo). Commercial samples of polysorbates were obtained from companies A–E via the Japan Food Additives Association. The NMR solvents, methanol-d_4 and acetone-d_6 with 0.03% tetramethylsilane (TMS), were purchased from Isotec Inc. (Miamisburg, OH). Potassium hydrogen phthalate (PHP), which was standard grade for volumetric analysis according to Japanese Industrial Standard (JIS) K8005, was purchased from Wako Pure Chemical Industries, Ltd.

Instrumentation

NMR spectra were recorded on JNM-ECA (500 MHz; JEOL, Tokyo) and MERCURY (400 MHz; VARIAN, Palo Alto, CA) pulsed Fourier-transform (FT) spectrometers, equipped with 5 mm $^1H\{X\}$ inverse detection gradient

Table I. Instruments and acquisition parameters.

Spectrometer	MERCURY400 (VARIAN) and ECA500 (JEOL)
Probe	5 mm indirect detection probe
Spectral width	2.5–12.5 ppm
Data points	64 000
Flip angle	45°
Pulse delay	30 s (>5 * T_1)
Scan times	8
Sample spin	15 Hz
Probe temperature	25°C
Solvent	Mixture of methanol-d_4 and acetone-d_6 (1:1)
Internal standard	Potassium hydrogen phthalate (PHP)
Range of integral signal	Oxyethylene group (EO) = 3.40–3.85 ppm 4 protons of PHP = 7.46–7.66 ppm + 8.18–8.38 ppm

probes, with methanol-d_4:acetone-d_6 (1:1) and 0.3% (w/v) PHP as an NMR solvent. The spectra were referenced internally to TMS by ^{1}H-NMR. The samples and internal standard were weighed on a LIBROR AEG-80SM (Shimadzu, Kyoto, Japan) electronic balance to an accuracy of ±0.01 mg.

Preparation of samples and NMR measurement conditions

The polysorbate samples were prepared as follows. PHP was crushed into a powder in a mortar and dried for 1 h at 120°C. After cooling in a desiccator, the powder (300 mg) was dissolved in 100 ml of methanol-d_4:acetone-d_6 (1:1) with ultrasonic agitation for 30 min. This stock solution was used as the NMR solvent and included an internal standard. A 50-mg polysorbate sample was then dissolved in 3 ml of the NMR solvent described above, and 0.6 ml of the sample solution was placed into a 5-mm NMR tube (Kusano Science Co. Ltd, Tokyo). The ^{1}H-NMR spectra were recorded on MERCURY400 and ECA500 spectrometers operating at 400 and 500 MHz, respectively. Typical ^{1}H-NMR parameters for the quantitative analyses are listed in Table I. The free induction decay (FID) signals of the samples from the MERCURY400 and ECA500 spectrometers were loaded onto a Windows XP-based personal computer (PC) equipped with the Alice 2 Version 5 (JEOL) NMR data-processing and analytical software. Fourier transformations of the FID signals were carried out with this software using the default parameters; window function = exponential, BF = 0.12 Hz, zero filling = 1, T1 = T2 = 0%, T3 = 90%, T4 = 100%. After phase adjustments and baseline corrections of the NMR spectra were performed using the same algorithms in the automatic mode of Alice 2, the signal intensities of the EOs and internal standard protons were measured, respectively.

Results and discussion

Identification of EO signals in polysorbates

Polysorbate molecules contain approximately 20 moles of EO according to the JECFA definition. However, recently reported matrix-assisted laser desorption/ionization time-of-flight mass spectrometry (MALDI-TOF MS) spectra showed that polysorbates include numerous other chemical species, including polyethylenes, unesterified, monoesterified, and diesterified polyoxyethylene sorbitans, and isosorbides (Frison-Norrie and Sporns 2001). Furthermore, analysis by liquid chromatography (LC)–mass spectrometry (MS) confirmed that polysorbates contain not only polyoxyethylene sorbitan fatty acid esters but also numerous intermediates, such as polyoxyethylene sorbitan and isosorbitan, and the monoesters and diesters of fatty acids (Vu Dang et al. 2006). These studies have confirmed that polysorbates comprise many types of chemical isomers. This molecular diversity makes it difficult to determine the EO contents of polysorbates. However, we hypothesized that the EO contents of polysorbates could be measured rapidly and simply by qNMR if the signals could be identified on ^{1}H-NMR spectra, regardless of whether they contained numerous chemical isomers.

Thus, in order to identify the EO signals in polysorbates, we compared the ^{1}H-NMR spectra of polysorbate 20, sorbitan monolaurate, and poly(ethylene glycol) distearate. The partial structures of sorbitan monolaurate and poly(ethylene glycol) distearate, which comprised a sorbitol anhydride core and poly(ethylene glycol), were similar to those of polysorbate 20 (Figures 2 and 3). The sorbitan monolaurate and poly(ethylene glycol) distearate spectra revealed fatty-acid moiety signals with δ_H values ranging from 0.9 to 2.4 ppm, similar to those of polysorbate 20. The triplet signal at $\delta_H c.$ 0.9 ppm, the major broad signal and multiplet signal at $\delta_H c.$ 1.3 ppm and 1.6 ppm, and the triplet signal at $\delta_H c.$ 2.4 ppm were identified as the terminal CH_3–, $-CH_2-$, and $-CH_2C{=}O-$ groups of the fatty acids, respectively. Most of the EO signals in poly(ethylene glycol) distearate were observed between δ_H values of 3.40 and 3.85 ppm. One of the $-CH_2O-$ groups appeared to have been shifted downfield to $\delta_H c.$ 4.2 ppm, near to the residual proton of methanol-d_4 at $\delta_H c.$ 4.4 ppm. A HMBC experiment revealed that the proton at $\delta_H c.$ 4.2 ppm was correlated to the carbonyl carbon of the fatty acid at δ_C 173.4 ppm. Thus, the proton signal was assigned

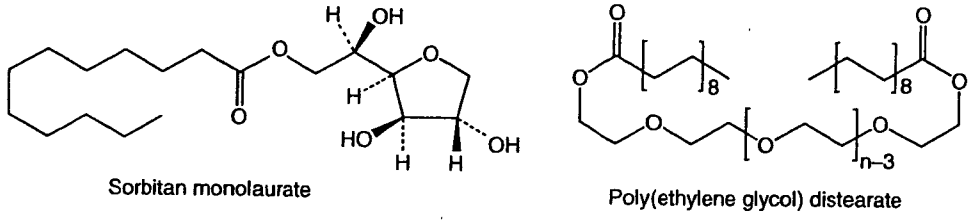

Figure 2. Structures of sorbitan monolaurate and poly(ethylene glycol) distearate.

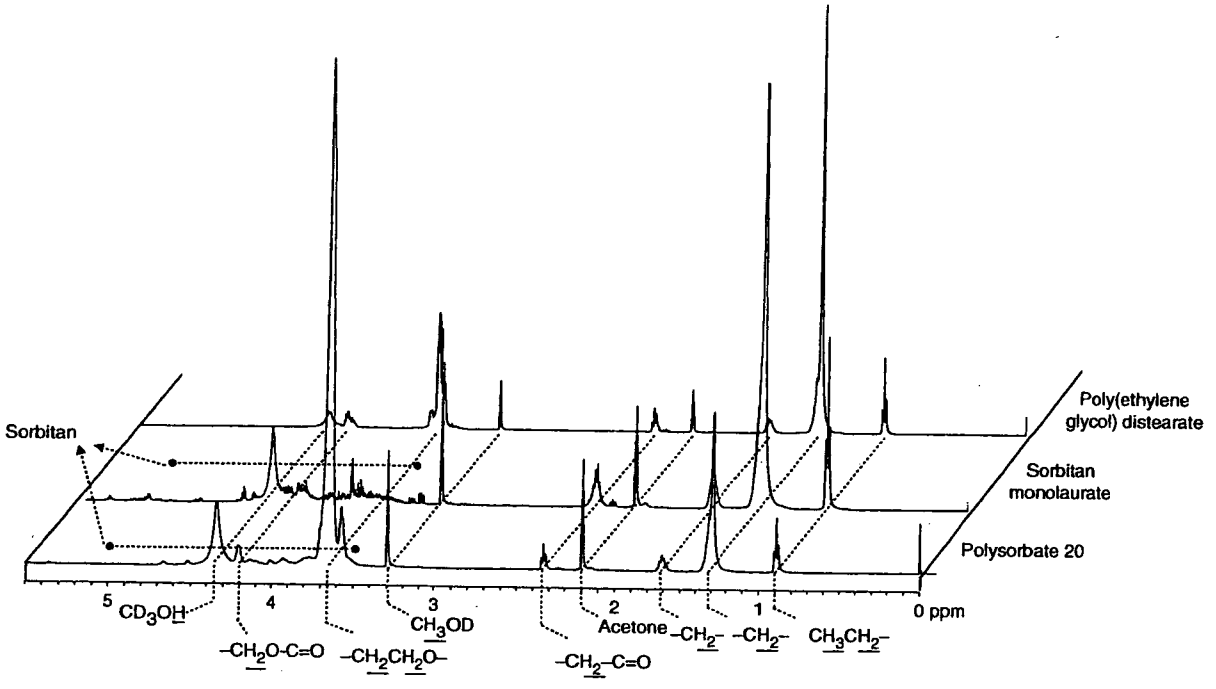

Figure 3. Comparison of NMR spectra of polysorbate 20, sorbitan monolaurate and poly(ethylene glycol) distearate. ^{1}H-NMR spectra were obtained using the ECA500 system (500 MHz; JEOL) under the conditions shown in Table I.

to the $-CH_2O-$ group adjacent to the fatty acid side chain. In the sorbitan monolaurate spectrum, various minor proton signals were observed from δ_H values of *c.* 3.4–5.0 ppm; these were attributed to the sorbitan moiety in sorbitan monolaurate, which consists of a mixture of cyclic sorbitol-derived ethers (such as sorbitan, isosorbite, and other isomers). These signals were also observed on the spectrum of polysorbate 20. However, the signals were broad and negligibly smaller than that of sorbitan monolaurate, as polysorbate 20 has the diversity of molecule more than sorbitan monolaurate. The polysorbate 20 signals ranging from δ_H 0.9 to 2.4 ppm that were attributed to the fatty-acid moiety were similar to those of sorbitan monostearate and poly(ethylene glycol) distearate. Polysorbate 60, 65, and 80 also showed the signals of fatty acid as same as sorbitan monolaurate, but the olefinic protons were only observed at δ_H 5.3 ppm on the spectrum of polysorbate 80 consisting of an unsaturated fatty acid (data not shown). The EO signals were assigned to a large envelop between δ_H 3.40 and 3.85 ppm, and at δ_H 4.20 ppm, which overlapped with the negligible small broad signals seen for the mixture of sorbitan, isosorbite, and other isomers moieties between δ_H values of *c.* 3.4 and 5.0 ppm. The EO signals of polysorbates 60, 65, and 80 also appeared within these ranges (data not shown). This was due to the fact that polysorbates basically comprise the same units: sorbitol anhydrides core, EO chains, and fatty acids. Although proton signals of the $-CH_2O-$ group adjacent to the fatty acid at δ_H *c.* 4.20 ppm were observed, and the signals of the sorbitol anhydrides core were overlapped on EO signals, they were negligible and did not effect the

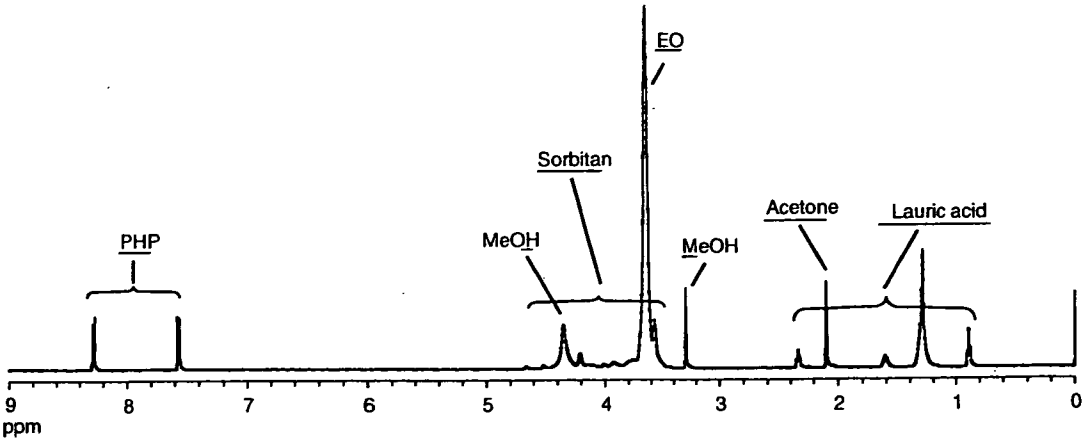

Figure 4. ^{1}H-NMR spectrum of polysorbate 20. The spectrum was obtained using the ECA500 system (500 MHz; JEOL). PHP was added as an internal standard. Signals of the four protons on the benzene ring of PHP were observed at δ_H values of 7.46–7.66 ppm and 8.18–8.38 ppm. Most of the EO signals of polysorbate 20 were observed in a large envelope between δ_H 3.40 and 3.85 ppm.

determination of the EO contents. Thus, in the current research, we used the EO signals between δ_H 3.40 and 3.85 ppm to determine the EO contents of polysorbates by NMR.

Determination of EO contents in polysorbates 20, 60, 65, and 80

Several reports have described the applications of qNMR to determine specific types of chemical compound, such as natural products, impurities, and polymers (Stefanova et al. 1988; Paula 2001; Jake et al. 2002; Wells et al. 2002; Paula et al. 2005). Recently, a practical set of parameters for qNMR has been discussed (Saito et al. 2004). Furthermore, qNMR using an internal standard has been suggested as a new way of determining the contents of surfactants with a relatively high throughput (Koike et al. 2004a, 2004b, 2005). To minimize quantitative errors, we used the qNMR conditions described by Koike and colleagues, as listed in Table I. In particular, the flip angle was set to 45°, and the spectral width was set at a value sufficient for the peak of interest to fall within 80% of its centre, because the signal intensities decreased towards both edges of the spectral window. The number of data points was set at 64 000 to enhance the resolution. The pulse delay was set at up to 30 s, as high-precision NMR can only be achieved when the pulse delay time is greater than the quintuple spin-lattice relaxation time ($>5 * T_1$). As qNMR is based on the fact that the signal intensities of a given resonance are directly proportional to the molar quantity of the nucleus within the sample, the EO signal intensity of polysorbates and four protons on the benzene ring of PHP were used to determine the EO contents. The total time taken to obtain one FID using these parameters was <10 min.

The weight percentage of the EO groups was calculated according to Equation 1.

$$\mathrm{EO(w/w\%)} = \frac{(I_{EO}/H_{EO} \times M_{EO}/W_{sample})}{(I_{standard}/H_{standard} \times M_{standard}/W_{standard})} \times 100. \quad (1)$$

Here, I_{EO} is the signal intensity of the EO group; H_{EO} is the number of protons of the EO group (four); M_{EO} is the partial molecular weight of the EO group (44); W_{sample} is the weight (mg) of the sample in 3 ml of NMR solvent including PHP as an internal standard; $I_{standard}$ is the total signal intensity of PHP; $H_{standard}$ is the number of protons on the benzene ring of PHP (four); $M_{standard}$ is the molecular weight of PHP (204); and $W_{standard}$ is the weight (mg) of PHP in 3 ml of NMR solvent.

We initially confirmed that the qNMR showed linearity between the intensity of the EO signal and the amount of polysorbate 20. Various amounts of the reagent-grade polysorbate 20 sample were analysed by ^{1}H-NMR under the conditions described in the Materials and methods and Table I. The NMR spectrum of polysorbate 20 with the internal standard is shown in Figure 4. The four protons of the PHP benzene ring were observed as two double–doublet signals at δ_H values of 7.46–7.66 ppm and 8.18–8.38 ppm, respectively. The ratio of the EO signal intensity was calculated as follows: intensity of EO/total intensities of four protons on PHP benzene ring. The relationship between EO/PHP and the amount of polysorbate 20 was linear ($R^2 = 0.9996$) in the range of 12.5–100 mg of polysorbate 20 in 3 ml of NMR solvent. Based on these results, we concluded

Table II. Determination of EO contents in polysorbates by qNMR.[a]

Sample name	MERCURY (400 MHz, VARIAN)			ECA500 (500 MHz, JEOL)		
	Entry	EO (%)	SD	Entry	EO (%)	SD
Polysorbate 20 (polyoxyethylene (20) sorbitan monolaurate)	1	73.0		1	72.2	
	2	71.8		2	71.8	
	3	73.2		3	72.3	
	4	71.7		4	72.5	
	5	71.9		5	71.6	
				6	72.9	
				7	72.0	
				8	72.7	
				9	73.7	
	AV	72.3	0.7	AV	72.4	0.6
Polysorbate 60 (polyoxyethylene (20) sorbitan monostearate)	1	67.7		1	67.4	
	2	65.3		2	67.7	
	3	68.9		3	67.5	
	4	67.8		4	67.9	
	5	66.9		5	68.6	
	AV	67.3	1.3	AV	67.8	0.5
Polysorbate 65 (polyoxyethylene(20) sorbitan tristearate)	1	49.1		1	49.8	
	2	49.8				
	3	49.5				
	4	49.8				
	5	48.7				
	AV	49.4	0.5			
Polysorbate 80 (polyoxyethylene (20) sorbitan monooleate)	1	65.0		1	67.0	
	2	65.5				
	3	66.2				
	4	64.8				
	5	65.1				
	AV	65.3	0.6			

[a]Reagent-grade polysorbates were purchased from Wako Pure Chemical Industries, Ltd. "Entry" means that the same sample was measured repeatedly on different days.

that qNMR could quantitatively determine the EO contents of polysorbates.

In order to verify whether qNMR could accurately determine the EO contents of polysorbates, two different NMR instruments (MERCURY and ECA500, with magnetic field strengths of 400 and 500 MHz, respectively) were used to repeatedly measure the EO contents of reagent grade polysorbates 20, 60, 65, and 80, which are generally used as standards. The results are shown in Table II. Reproducible results were obtained from each sample using the MERCURY system. Furthermore, the results obtained by the two NMR instruments did not differ significantly (standard deviations = 0.5–1.3%). These findings confirmed that it was possible to determine the EO contents of polysorbates using this approach regardless of the NMR instrument employed.

Finally, to confirm the validity of qNMR, we determined the EO contents of the commercially synthesized polysorbates 20, 60, 65, and 80, which met the specifications of the JECFA. All of the EO contents of the polysorbates were within the limits described in the *Compendium of Food Additive and Flavoring Agent Specifications* (JECFA [internet]) (Table III). The qNMR method for determining the EO contents of polysorbates demonstrated in this paper thus represents a simple and rapid alternative to the classic titration method recommended by the JECFA, which does not require specific chemical reactions or sophisticated apparatus. Moreover, the qNMR method made it possible to distinguish between Polysorbates 60 and 80, which have the same stipulated value, by comparison with the ^{1}H-NMR spectra, as polysorbate 80 consisting of an unsaturated fatty acid only showed the signals of olefinic protons at δ_H 5.3 ppm. It is theoretically possible to determine the ratio of a substituted group in any molecule, or the quality of any compound, using the proposed qNMR method with an internal standard, provided that the target proton signals can be separated from those

Table III. EO contents in commercial polysorbates determined using qNMR.[a]

Name	Stipulated value	Brand	EO (%)	SD
Polysorbate 20 (polyoxyethylene (20) sorbitan monolaurate)	70.0–74.0%	A	71.2	
		B	73.0	
		C	70.3	
		D	71.0	
		E	71.5	
		AV	71.4	1.0
Polysorbate 60 (polyoxyethylene (20) sorbitan monostearate)	65.0–69.5%	A	66.9	
		B	65.4	
		C	68.0	
		D	68.1	
		E	67.2	
		AV	67.1	1.1
Polysorbate 65 (polyoxyethylene (20) sorbitan tristearate)	46.0–50.0%	A	48.3	
		B	46.0	
		C	-	
		D	47.2	
		E	48.1	
		AV	47.4	1.1
Polysorbate 80 (polyoxyethylene (20) sorbitan monooleate)	65.0–69.5%	A	67.4	
		B	65.1	
		C	69.3	
		D	66.7	
		E	68.0	
		AV	67.1	1.6

[a]Brands A–E were purchased from five manufacturers. Brand C does not supply polysorbate 65.

of non-target groups and impurities. We are currently investigating the potential for this technique to determine various other compounds and polymers.

Conclusions

This research demonstrated that the EO contents of commercial polysorbates 20, 60, 65, and 80 could be readily determined using qNMR with an internal standard. Clear NMR data for the polysorbates were obtained from simple sample preparations. Two different NMR instruments validated the proposed method, and no significant differences were observed among the results. Moreover, the data obtained for commercial polysorbates 20, 60, 65, and 80 were in good agreement with the JECFA guidelines.

It is generally difficult to determine the amounts of substituted groups within polymers owing to their great diversity in molecular weights and structures. Classical methods require time-consuming preparation to set up the apparatus, and technically skilled operators. Furthermore, as there are no alternative methods to validate the results, they have to be accepted without verification. Our proposed qNMR is a rapid and simple analysis that provides the structural information of target compounds together. These advantages will reduce dramatically the time and manpower cost required, even if the NMR spectrometer and the solvents are expensive. qNMR is thus a valuable additional and/or alternative method, with a broad range of applications in quantitative analysis.

Acknowledgements

This work was supported by a Research on Food Safety in Health and Labour Sciences Research Grants from the Ministry of Health, Labor, and Welfare of Japan.

References

Frison-Norrie S, Sporns P. 2001. Investigating the molecular heterogeneity of polysorbate emulsifiers by MALDI-TOF MS. Journal of Agricultural and Food Chemistry 49:3335–3340.

Jake B, Sticher O, Veit M, Fröhlich R, Paili GF. 2002. Evaluation of glucoiberin reference material from Iberis amara by spectroscopic fingerprinting. Journal of Natural Products 65:517–522.

Jancke H. 1998. NMR spectroscopy as a primary analytical method. Comité Consultatif pour la Quantité de Matière Report 98: 1–12.

Joint FAO/WHO Expert Committee on Food Additives (JECFA). Available: http://www.fao.org/ag/agn/jecfa/archive_en.stm. Accessed 20 November 2006.

Koike R, Jo S, Azuma M, Wakisaka T. 2004a. Precise and rapid determination of anionic and cationic surfactants by ^{1}H nuclear magnetic resonance using an internal standard. Bunseki Kagaku (The Japan Society for Analytical Chemistry) 53:1125–1131.

Koike R, Jo S, Azuma M, Wakisaka T. 2004b. Precise and rapid determination of amphoteric and nonionic surfactants by ^{1}H nuclear magnetic resonance using an internal standard. Bunseki Kagaku (The Japan Society for Analytical Chemistry) 53:1133–1138.

Koike R, Jo S, Azuma M, Wakisaka T. 2005. Precise and simultaneous determination of surfactants by ^{1}H nuclear magnetic resonance using an internal standard. Bunseki Kagaku (The Japan Society for Analytical Chemistry) 54:715–722.

Paula GF. 2001. qNMR—a versatile concept for the validation of natural product reference compounds. Phytochemical Analysis 12:28–42.

Paula GF, Jake BU, Lankin DC. 2005. Quantitative ^{1}H NMR: Development and potential of a method for natural products analysis. Journal of Natural Products 68:133–149.

Saito T, Ihara T, Sato H, Jancke H, Kinugasa S. 2003. International comparison on the determination of an ethanol aqueous solution by ^{1}H nuclear magnetic resonance. Bunsaki Kagaku (The Japan Society for Analytical Chemistry) 52:1029–1036.

Saito T, Nakaie S, Kinoshita M, Ihara T, Kinugasa S, Nomura A, Maeda T. 2004. Practical guide for accurate quantitative solution state NMR analysis. Metrologia 41:213–218.

Stefanova R, Rankoff D, Panayotova S, Spassov SL. 1988. Quantitative proton NMR determination of linoleic acid mono- and diester of polyethyleneglycols via reaction with trichloroacetyl isocyanate. Journal of American Oil Chemists' Society 65:1516–1518.

Vu Dang HV, Gray AI, Watson D, Bates CD, Scholes P, Gillian GM. 2006. Composition analysis of two batches of polysorbate 60 using MS and NMR techniques. Journal of Pharmaceutical and Biomedical Analysis 40:1155–1165.

Wells RJ, Hook JM, Al-Deen TS, Hibbert DB. 2002. Quantitative nuclear magnetic resonance (QNMR) spectroscopy for assessing the purity of technical grade agrochemicals: 2,4-Dichlorophenoxyacetic acid (2,4-D) and sodium 2,2-dichloropropionate (dalapon sodium). Journal of Agricultural and Food Chemistry 50:3366–3374.